New Skyrme energy density functional for a better description of charge-exchange resonances

Xavier Roca-Maza[1], Gianluca Colò[1,2], and Hiroyuki Sagawa[3,4]

[1] *INFN, Sezione di Milano, Via Celoria 16, I-20133, Milano Italy*

[2] *Dipartimento di Fisica, Università degli Studi di Milano, via Celoria 16, I-20133 Milano, Italy*

[3] *Center for Mathematics and Physics, University of Aizu, Aizu-Wakamatsu, Fukushima 965-8560, Japan*

[4] *Nishina Center, Wako, Saitama 351-0198, Japan*

Phys. Rev. **C 86 031306(R) 2012**

19^{th} Nuclear Physics Workshop

"Marie & Pierre Curie" Kazimierz 2012

Table of contents:

Motivation:

Spin-isospin properties

- **Skyrme HF+RPA enables an effective description of the nuclear many-body problem**
- **Open problems need to be understood and eventually solved**
  - **Accurate determination** of the **spin-isospin properties** of the Skyrme effective interaction $\Rightarrow$ **accurate description** of charge exchange excitations such as the **Gamow Teller Resonance**
- **Gamow Teller**
  - transitions govern electron capture during the core-colapse of supernovæ
  - matrix el. are necessary for the study of **double-β decay** (in neutrinoless double-β decay is crucial for a precise determination of the neutrino mass).
  - matrix el. may be useful in the **calibration of detectors used to measure electron-neutrinos** coming from the Sun

Motivation:

Gamow Teller Resonance I

Neither the strength nor the E_x properly described in HF+RPA

- SGII[a] $\Rightarrow$ earliest attempt to give a quantitative description of the GTR
- SkO'[b] $\Rightarrow$ accurate in ground state finite nuclear properties and improves the GTR
- Relativistic MF and Relativistic HF (PKO1[c]) calculations are also available

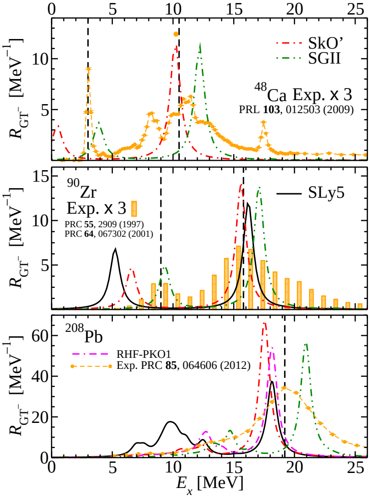

[a] N. Giai and H. Sagawa, Phys. Lett. B **106**, 379 (1981), [b] P.-G. Reinhard et al., Phys. Rev. C **60**, 014316 (1999), [c] H. Liang, N. Van Giai, and J. Meng, Phys. Rev. Lett. **101**, 122502 (2008), SLy5 – E. Chabanat et al., Nucl. Phys. A **635**, 231 (1998); E. Chabanat *et al.*, ibid. **643**, 441 (1998)

Motivation:

Gamow Teller Resonance II: quenching of the strength

- **Experimentally**, the **GTR** exhausts **60–70%** of the **Ikeda sum rule**: $\int [R_{\mathrm{GT}^-}(E) - R_{\mathrm{GT}^+}(E)]dE = 3(N - Z)$
- To **explain** the problem, two possibilities that go beyond RPA correlations have been drawn:
  - the effects of the second-order configuration mixing: **2p-2h correlations**
  - within the quark model, a **n(p)** can become a **p(n)** or a $\Delta^+(\Delta^{++})$ under the action of the GT$^-$ operator and since there is **no Pauli blocking for Δ−h excitations** $\Rightarrow$ it may **contribute to the GTR**.
- The **experimental analysis of ^{90}Zr** $\Rightarrow$ **quenching** (2/3) has to be **mainly attributed to 2p-2h** coupling and not to Δ−isobar effects much smaller [T. Wakasa *et. al.*, Phys. Rev. C **55**, 2909 (1997)].
- E_x **GTR in nuclei** mainly in the region of several **tens of MeV** and the Δ−h states are hundreds of MeV above the GT $\Rightarrow$ **hard to excite the Δ** in the nuclear medium.

Motivation:

Which gs properties are important for describing the E_x^{GTR}?

A recent study[a] on the GTR and the spin-isospin Landau-Migdal parameter G_0' using several Skyrme sets,

- concluded that G_0' **is not the only important quantity** in determining the **excitation energy of the GTR** in nuclei
- **spin-orbit splittings** also influences the GTR

- Empirical indications[b] suggest that $G_0' > G_0 > 0$
- **Not a very common feature** within available Skyrme forces[c]

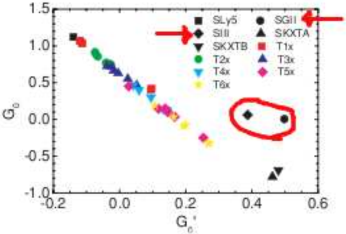

[a] M. Bender, J. Dobaczewski, J. Engel, and W. Nazarewicz, Phys. Rev. C **65**, 054322 (2002); [b] T. Wakasa, M. Ichimura, and H. Sakai, Phys. Rev. C **72**, 067303 (2005); T. Suzuki and H. Sakai, Phys. Lett. B **455**, 25 (1999), [c] Li-Gang Cao, G. Colo, and H. Sagawa, Phys. Rev. C **81**, 044302 (2010)

Why spin-orbit splittings are important?

$E_x^1 \approx \epsilon_{\pi 1g_{7/2}} - \epsilon_{\nu 1g_{9/2}} + \epsilon_{\mathrm{ph}}^1$
$E_x^2 \approx \epsilon_{\pi 1g_{9/2}} - \epsilon_{\nu 1g_{9/2}} + \epsilon_{\mathrm{ph}}^2$
$\Delta E_x \approx \boldsymbol{\Delta}\epsilon_{\pi \mathbf{1g}} + \Delta\epsilon_{\mathrm{ph}}$

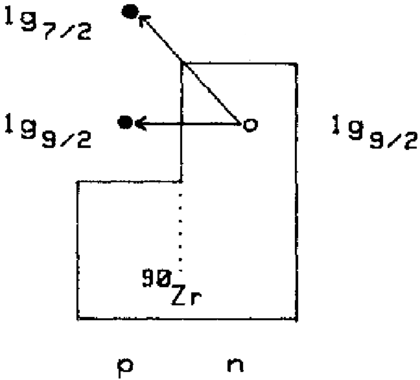

Schematic picture of single-particle transitions involved in the Gamow Teller Resonance of ^{90}Zr. Transitions excited by $\sigma\tau_-$ operator.

F. Osterfeld, Rev. Mod. Phys. **64**, 491 (1992)

Skyrme Model

Hamiltonian[a]

Includes **central tensor terms (J^2 terms)** due to the coupling of tensor and spin and gradients terms and **two spin-orbit parameters** (same as SkO and some SkI forces)

$$\mathcal{H} = \mathcal{K} + \mathcal{H}_0 + \mathcal{H}_3 + \mathcal{H}_{\rm eff} + \mathcal{H}_{\rm fin} + \mathcal{H}_{\rm SO} + \mathcal{H}_{\rm sg} + \mathcal{H}_{\rm Coul}$$

$$\begin{aligned}
\mathcal{K} &= \hbar^2\tau/2m \\
\mathcal{H}_0 &= (1/4)t_0[(2+x_0)\rho^2 - (2x_0+1)(\rho_n^2+\rho_p^2)] \\
\mathcal{H}_3 &= (1/24)t_3\rho^\alpha[(2+x_3)\rho^2 - (2x_3+1)(\rho_n^2+\rho_p^2)] \\
\mathcal{H}_{\rm eff} &= (1/8)[t_1(2+x_1)+t_2(2+x_2)]\tau\rho \\
&\quad + (1/8)[t_2(2x_2+1)-t_1(2x_1+1)](\tau_n\rho_n+\tau_p\rho_p) \\
\mathcal{H}_{\rm fin} &= (1/32)[3t_1(2+x_1)-t_2(2+x_2)](\nabla\rho)^2 \\
&\quad - (1/32)[3t_1(2x_1+1)+t_2(2x_2+1)][(\nabla\rho_n)^2+(\nabla\rho_p)^2] \\
\mathcal{H}_{\rm SO} &= (1/2)W_0\mathbf{J}\cdot\nabla\rho + (1/2)W_0'(\mathbf{J}\cdot_{\mathbf{n}}\nabla\rho_n + \mathbf{J_p}\cdot\nabla\rho_p) \\
\mathcal{H}_{\rm sg} &= -(1/16)(t_1x_1+t_2x_2)\mathbf{J}^2 + (1/16)(t_1-t_2)(\mathbf{J_n}^2+\mathbf{J_p}^2)
\end{aligned}$$

[a] E. Chabanat et al., Nucl. Phys. A **635**, 231 (1998); E. Chabanat *et al.*, ibid. **643**, 441 (1998)

Fitting Protocol

χ^2 **definition:** $\chi^2 = \frac{1}{N_{\mathrm{data}}} \sum_i^{N_{\mathrm{data}}} \frac{(\mathcal{O}_i^{\mathrm{theo.}} - \mathcal{O}_i^{\mathrm{data}})^2}{(\Delta \mathcal{O}_i^{\mathrm{data}})^2}$

Landau-Migdal parameters in infinite nuclear matter G_0 and G_0' fixed to **0.15** and **0.35**, respectively, at ρ_0.

Table: Data and *pseudo*-data $\mathcal{O}_i$, adopted errors for the fit $\Delta\mathcal{O}_i$ and selected finite nuclei and EoS.

$\mathcal{O}_i$	$\Delta\mathcal{O}_i$	
B	1.00 MeV	^{40,48}Ca, ^{90}Zr, ^{132}Sn and ^{208}Pb
r_c	0.01 fm	^{40,48}Ca, ^{90}Zr and ^{208}Pb
ΔE_{SO}	$0.04\times\mathcal{O}_i$	$\pi 1g$ in ^{90}Zr and $\pi 2f$ in ^{208}Pb
$e_n(\rho)$	$0.20\times\mathcal{O}_i$	R. B. Wiringa *et al.*, PRC **38**, 1010 (1988)

Skyrme Aizu Milano interaction: SAMi

Parameter set and nuclear matter properties:

Table: SAMi parameter set and saturation properties with the estimated standard deviations inside parenthesis

	value(σ)			value(σ)	
t_0	$-1877.75(75)$	MeV fm^3	ρ_∞	0.159(1)	fm^{-3}
t_1	475.6(1.4)	MeV fm^5	e_∞	$-15.93(9)$	MeV
t_2	$-85.2(1.0)$	MeV fm^5	m^*_{IS}	0.6752(3)	
t_3	10219.6(7.6)	MeV fm$^{3+3\alpha}$	m^*_{IV}	0.664(13)	
x_0	0.320(16)		J	28(1)	MeV
x_1	$-0.532(70)$		L	44(7)	MeV
x_2	$-0.014(15)$		K_∞	245(1)	MeV
x_3	0.688(30)		G_0	0.15	(fixed)
W_0	137(11)		G_0'	0.35	(fixed)
W_0'	42(22)				
α	0.25614(37)				

SAMi: spin and spin-isospin instabilities in NM

Imposing that spin and isospin dof at the Fermi surface are stable under generalized deformations [S.-O. Bäckman *et al.*, Nucl. Phys. A **321**, 10 (1979)]

$$1 + G_0 > 0 \qquad 1 + G_0' > 0$$

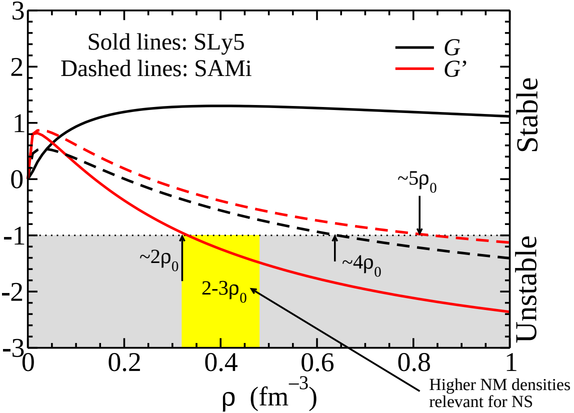

Results

Equation of State: SAMi vs *ab*–initio calculations

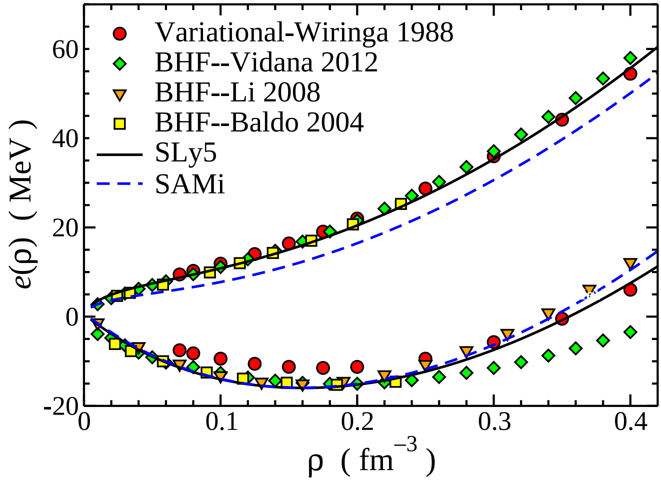

Figure: Neutron and symmetric matter EoS as predicted by the HF SAMi (dashed line) and SLy5 (solid line) interactions and by the benchmark microscopic calculations of R. B. Wiringa *et al.*, PRC **38**, 1010 (1988) (circles). State-of-the-art BHF calculations are shown by diamonds I. Vidaña, private communication, triangles Z. H. Li *et al.*, Phys. Rev. C **77**, 034316 (2008) and squares M. Baldo *et al.*, Nucl. Phys. A **736**, 241 (2004).

Results

Finite Nulcei: spherical double-magic nuclei

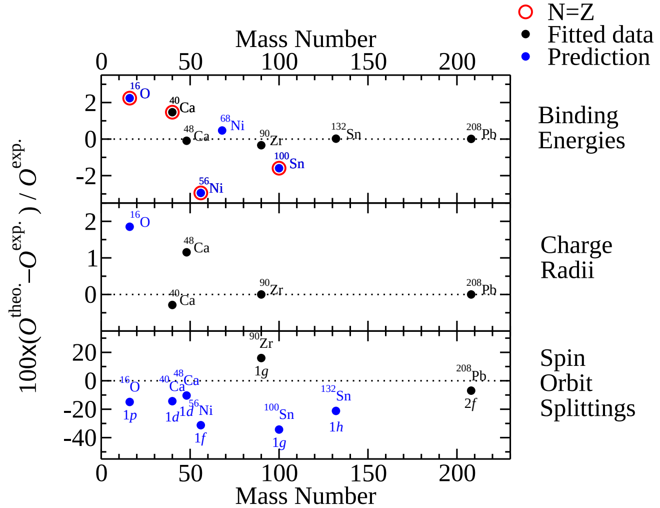

Figure: Finite nuclei properties as predicted by the HF SAMi (black circles) and some predictions (blue circles) for spherical double-magic nuclei. Experimental data taken from Refs. G. Audi *et al.*, NPA **729**, 337 (2003), I. Angeli, ADNDT **87**, 185 (2004), M. Zalewski *et al.*, PRC **77**, 024316 (2008)

Results

Giant Monopole and Dipole Resonances in ^{208}Pb

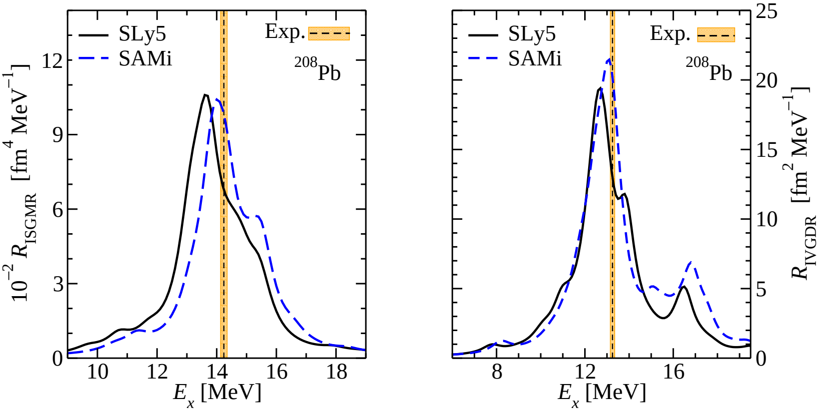

Figure: Strength function at the relevant excitation energies in ^{208}Pb as predicted by SLy5 and the SAMi interaction for GMR and GDR. A Lorentzian smearing parameter equal to 1 MeV is used. Experimental data for the centroid energies are also shown: $E_c(GMR) = 14.24 \pm 0.11$ MeV [D. H. Youngblood, et al., Phys. Rev. Lett. **82**, 691 (1999)] and $E_c(GDR) = 13.25 \pm 0.10$ MeV [N. Ryezayeva et al., Phys. Rev. Lett. **89**, 272502 (2002)].

Results

Gamow Teller Resonance in ^{48}Ca, ^{90}Zr and ^{208}Pb

Operator:
$\sum_{i=1}^{A} \sigma(i)\tau_{\pm}(i)$

Figure: Gamow Teller strength distributions in ^{48}Ca (upper panel), ^{90}Zr (middle panel) and ^{208}Pb (lower panel) as measured in the experiment [T. Wakasa *et al.*, Phys. Rev. C **55**, 2909 (1997), K. Yako *et al.*, Phys. Rev. Lett. **103**, 012503 (2009), A. Krasznaborkay *et al.*, Phys. Rev. C **64**, 067302 (2001), H. Akimune *et al.*, Phys. Rev. C **52**, 604 (1995) and T. Wakasa et al., Phys. Rev. C **85**, 064606 (2012)] and predicted by SLy5, SkO', SGII and SAMi forces.

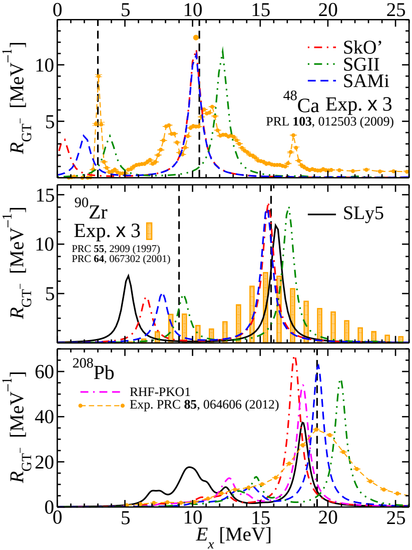

Results

Spin Dipole Resonances in ^{90}Zr and ^{208}Pb

Operator:

$$\sum_{i=1}^{A} \sum_{M} \tau_{\pm}(i) r_i^L \left[Y_L(\hat{r}_i) \otimes \sigma(i)\right]_{JM}$$

Sum Rule:

$$\int [R_{\mathrm{SD}^-}(E) - R_{\mathrm{SD}^+}(E)]\mathrm{d}E = \frac{9}{4\pi}\left(N\langle r_n^2\rangle - Z\langle r_p^2\rangle\right)$$

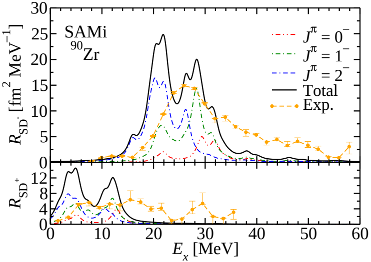

Figure: Spin Dipole strength distributions in ^{90}Zr as a function of the excitation energy E_x in the τ_- channel (upper panel) and τ_+ channel (lower panel) measured in the experiment [K. Yako *et al.*, Phys. Rev. C **74**, 051303(R) (2006)] and predicted by SAMi. Multipole decomposition is also shown. A Lorentzian smearing parameter equal to 2 MeV is used.

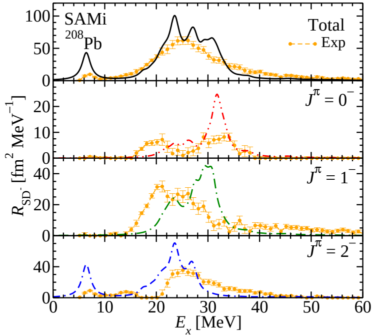

Figure: SDR strength distributions for ^{208}Pb in the τ_- channel from experiment [T. Wakasa *et al.*, Phys. Rev. C **85**, 064606 (2012)] and SAMi calculations. Total and multipole decomposition of the SDR strength are shown: total (upper panel), $J^\pi = 0^-$ (middle-upper panel), $J^\pi = 1^-$ (middle-lower panel) and $J^\pi = 2^-$ (lower panel). A Lorentzian smearing parameter equal to 2 MeV is used.

Conclusions:

- we have **successfully determined a new Skyrme** energy density functional which **accounts** for the most relevant quantities in order to improve the description of **charge-exchange nuclear resonances**:
  - the **hierarchy** and **positive values** of the spin and spin-isospin Landau-Migdal parameters G_0 **and** G_0'
  - the **proton spin-orbit splittings** of different **high angular momenta** single-particle levels
- the **GTR** in ^{48}Ca and the **GTR**, **IAR**, and **SDR** in ^{90}**Zr** and ^{208}**Pb** are predicted with **good accuracy by SAMi**
- **SAMi** does **not deteriorate** the description of other **nuclear observables**
- **applicability in nuclear physics and astrophysics**

Thank you for your attention!

Extra Material

Landau-Migdal vs Skyrme parameters

- **Within LDA**, at each density of the nucleus, $V_{\rm ph} \approx V$ nuclear matter having the same density
- Bulk properties of nuclear matter $\Rightarrow$ two-body interaction at the Fermi surface.
  $\langle \mathbf{k_1 k_2} | V | \mathbf{k_1 k_2} \rangle = ...$ (1)
- The p-h interaction at the Fermi surface is derived as the second functional derivative of the total energy with respect to density at the Fermi surface.
  $V_{\rm ph} = \sum_{\alpha=1,\tau,\sigma,\tau\cdot\sigma} \frac{\delta \mathcal{H}}{\delta\rho_\alpha \delta\rho_\alpha} =$
  $N_0^{-1}(F + F'\tau_\mathbf{1}\tau_\mathbf{2} + G\sigma_\mathbf{1}\sigma_\mathbf{2} + G'\tau_\mathbf{1}\tau_\mathbf{2}\sigma_\mathbf{1}\sigma_\mathbf{2})$ (2)
- Comparing **Eqs. 1** and **2** one finds the relation between the Landau-Migdal and the Skyrme parameters: $\mathbf{G_0} N_0 =$
  $-\frac{1}{4}t_0 + \frac{1}{2}t_0x_0 - \frac{1}{8}t_1k_{\rm F}^2 + \frac{1}{4}t_1x_1k_{\rm F}^2 + \frac{1}{8}t_2k_{\rm F}^2 + \frac{1}{4}t_2x_2k_{\rm F}^2 - \frac{1}{24}t_3\rho^\alpha + \frac{1}{12}t_3x_3\rho^\alpha$
  $\mathbf{G'_0} N_0 = -\frac{1}{4}t_0 - \frac{1}{8}t_1k_{\rm F}^2 + \frac{1}{8}t_2k_{\rm F}^2 - \frac{1}{24}t_3\rho^\alpha$

  $N_0 = 2k_{\rm F}m^*/\hbar^2\pi^2$ is the density of states

Note: $\mathbf{k_1}$ and $\mathbf{k_2}$ are taken at the Fermi surface and, therefore, in homogeneous nuclear matter the Landau parameters are only functions of the angle between them and the Fermi momentum.

Empirical constraints on G_0 and G_0'

- **Gamow-Teller Resonance** using RPA based on the Woods-Saxon potential have been studied and the **Landau-Migdal parameters estimated by comparing experiment** with theoretical calculations in Refs. [T. Wakasa, M. Ichimura, and H. Sakai, Phys. Rev. C **72**, 067303 (2005) and T. Suzuki and H. Sakai, Phys. Lett. B **455**, 25 (1999)].
  - Landau-Migdal parameter **G_0'(N−N) dominates the excitation energy in the GTR** as compared the contribution of to G_0'(N−Δ).
  - **G_0'(N−Δ) influences more the quenching**
- In our fit, **we do not use the obtained values as pseudodata** because **our theoretical framework is different and the results are associated to different m^*** (our sp energies are based on HF calculations instead of a Wood-Saxon potential).
- **We use** the empirical result in which an **hierarchy** between spin and spin-isospin parameters is suggested:

$$G_0' > G_0 > 0$$

Covariance analysis: χ^2 test

Observables $\mathcal{O}$ are used to calibrate the parameters $\mathbf{p}$ of a given model. The optimum parametrization $\mathbf{p}_0$ is determined by a least-squares fit with the global quality measure,

$$\chi^2(\mathbf{p}) = \sum_{\imath=1}^{m} \left(\frac{\mathcal{O}_\imath^{\mathrm{theo.}} - \mathcal{O}_\imath^{\mathrm{ref.}}}{\Delta \mathcal{O}_\imath^{\mathrm{ref.}}} \right)^2$$

Assuming that the χ^2 is a well behaved (analytical) function in the vicinity of the minimum and that can be approximated by an hyper-parabola,

$$\begin{aligned} \chi^2(\mathbf{p}) - \chi^2(\mathbf{p}_0) &\approx \frac{1}{2} \sum_{\imath,\jmath}^{n} (p_\imath - p_{0\imath}) \partial_{p_\imath} \partial_{p_\jmath} \chi^2 (p_\jmath - p_{0\jmath}) \\ &\equiv \sum_{\imath,\jmath}^{n} (p_\imath - p_{0\imath}) \mathcal{M}_{\imath\jmath} (p_\jmath - p_{0\jmath}) \end{aligned}$$

where $\mathcal{M}$ is the curvature matrix.

Covariance analysis: χ^2 test

$\mathcal{M}$ provides us access to estimate the errors between predicted observables ($A(\mathbf{p})$),

$$\Delta\mathcal{A} = \sqrt{\sum_{\imath}^{n} \partial_{p_\imath} A \mathcal{E}_{\imath\imath} \partial_{p_\imath} A} \tag{1}$$

$\mathcal{E} = \mathcal{M}^{-1}$ and the correlations between predicted observables,

$$c_{AB} \equiv \frac{C_{AB}}{\sqrt{C_{AA} C_{BB}}} \tag{2}$$

where,

$$C_{AB} = \overline{(A(\mathbf{p}) - \overline{A})(B(\mathbf{p}) - \overline{B})} \approx \sum_{\imath\jmath}^{n} \partial_{p_\imath} A \mathcal{E}_{\imath\jmath} \partial_{p_\jmath} B$$

Covariance analysis: SLy5-min as an example

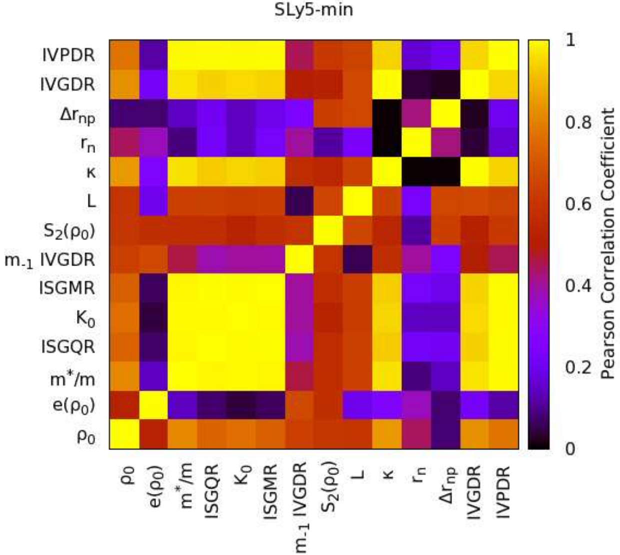

Covariance analysis: SLy5-min as an example

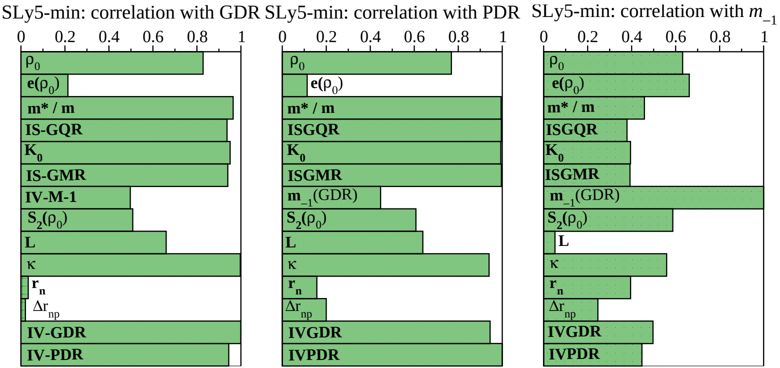

Figure: Pearson product-moment correlation coefficient for the IVGDR (left panel), IVPDR (middle panel) and m_{-1}(IVGDR) (right panel) with all other studied properties as predicted by the covariance analysis of SLy5.